Journal of Applied Polymer Science

The Influence of Molar Mass on Rheological and Dilute Solution Properties of Poly(butylene succinate)

Matthieu Garin,[1] Lan Tighzert,[1] Isabelle Vroman,[1] Sinisa Marinkovic,[2] Boris Estrine[2]

[1]Laboratoire LISM, UFR Sciences Exactes et Naturelles, BATIMENT 6, Moulin de la Housse, BP 1039, 51687 Reims Cedex 2, France

[2]Agro-Industries Recherches et Développements (ARD), Route de Bazancourt, 51110 Pomacle, France

Correspondence to: M. Garin (E-mail: matthieu.garin8@gmail.com)

ABSTRACT: The fundamental rheological properties of a wide molar mass M_w range of poly(butylene succinate)s (PBSs) are investigated. For entangled samples and a reference temperature of 140°C, the shear viscosity is described by the Carreau–Yasuda model. The plateau modulus is estimated at 1.5×10^5 Pa, the average activation energy of PBS melt is $\bar{E}_a = 45.02 \pm 3.09$ kJ mol^{-1}, and the critical molar mass for entanglement M_c is found to be 16,000 g mol^{-1} (PS equivalent). The dilute solution properties of PBS are also studied. A size exclusion chromatography equipped with a triple detection system is used to estimate the Mark–Houwink–Sakurada (MHS) parameters of PBS in solution in chloroform at 30°C. The exponent a and the coefficient K of the MHS relationship are found to be 0.71 ± 0.1 and $39.94 \times 10^{-5} \pm 6.31 \times 10^{-5}$ dL g^{-1}(g mol^{-1})$^{-a}$, respectively. © 2014 Wiley Periodicals, Inc. J. Appl. Polym. Sci. **2014**, *131*, 40887.

KEYWORDS: biodegradable; biopolymers and renewable polymers; polyesters; rheology; viscosity and viscoelasticity

Received 5 March 2014; accepted 17 April 2014

DOI: 10.1002/app.40887

INTRODUCTION

Currently, the polymer and materials industries face two significant challenges: fossil resource depletion and waste management. Concerning the latter, one solution involves incinerating plastic waste, thereby converting it to energy. An alternative solution would be to recycle plastic waste.[1] While recycling is attractive from an environmental standpoint, incineration is not due to its significant contribution to greenhouse gas emissions. The research sector of the plastics industry has actively pursued the development of natural and synthetic biodegradable polymers derived from renewable resources, as biodegradability offers an attractive alternative to incineration by transforming polymers into biomass.[2,3]

Among biodegradable polyesters based on agro-resources such as poly(lactic acid) and poly(hydroxyalkanoate)s, poly(butylene succinate) (PBS) is of great interest as a replacement for polyolefins such as polyethylene or polypropylene. In addition to its desirable physical–chemical properties (biodegradability, mechanical and thermal properties, processability, etc.), another advantage of PBS lies in the origin of its two monomers: succinic acid (SA) and 1,4-butanediol (BDO). In fact, the biotechnological route to obtaining SA from fungi, yeast, and bacterial strains was first explored a few decades ago.[4,5] More recently, an intensive research effort has focused on natural bacterial strains such as *Anaerobiospirillum succiniciproducens*, *Actinobacillus succinogenes*, *Mannheimia succiniciproducens*, and on recombinant *Escherichia coli* in order to improve SA production yields.[6–9] In spite of the fossil fuel origin of the major part of BDO production, this second monomer can also be biosourced. For example, BDO can be synthesized by reduction of SA or succinic anhydride.[9–11] Genomatica recently reported that recombinant *E. Coli* is capable of producing BDO from glucose.[12]

Although the general literature on PBS is extensive, there is an obvious lack of information about fundamental rheological properties of PBS, such as critical molar mass M_c, plateau modulus, or PBS melt activation energy E_a. Indeed, most articles describing PBS rheological properties are about high molar PBS,[13,14] PBS nanocomposites,[15–19] PBS blended with other polymers,[20,21] or PBS foam.[22] Thus, our findings on the influence of molar mass on PBS rheological properties are reported in the first part of this study.

Mark–Houwink–Sakurada (MHS) parameters of PBS in solution in chloroform are reported in the second part of this study, as no reference reporting these values could be found in

Additional Supporting Information may be found in the online version of this article.

Table I. Molecular Characteristics, Parameters of the Carreau-Yasuda Relationship, and Zero-Shear Viscosity from (2) of PBS Samples at 140°C

Sample	PBSa	PBSb	PBSc	PBSd	PBSe	PBSf	PBSg	PBSh	PBSi
M_w (g mol^{-1}) (PS eq.)	4000	6000	23,800	88,800	99,700	109,400	122,400	146,400	155,400
I_p[a]	1.5	1.9	1.83	2.16	2.24	2.27	2.23	2.4	2.47
η_0 (Pa s)[b] (From (2))	0.079	0.188	1.16	129	230	297	330	1410	1960
η_0 (Pa s)[c] (from C-Y)	-	-	-	129	228	298	330	1444	2066
λ (s)[d]	-	-	-	0.024	0.034	0.05	0.049	0.251	0.328
m[d]	-	-	-	0.83	0.72	0.73	0.71	0.61	0.58
a[d]	-	-	-	1.39	1.08	1.12	1.09	0.82	0.78

[a] Polymolecularity index of PBS samples.
[b] Zero-shear viscosity determined from eq. (2).
[c] Zero-shear viscosity determined from the Carreau-Yasuda relationship.
[d] Parameters of the Carreau-Yasuda relationship (1).

literature. The estimation of these parameters is very useful as M_w evolution can be monitored during polymerization or degradation of a polymer by solution viscosity measurements. We chose chloroform because it is widely used as a PBS solvent.

EXPERIMENTAL

Materials

BDO (99%), SA (99%), titanium (IV) butoxide (TBT) (97%), and chloroform solvent (Sigma-Aldrich, 99.8%) were purchased from Sigma-Aldrich and used without further purification.

Synthesis of PBS

About 0.15 mol of SA and desired amounts of BDO and TBT were charged in a 250-mL glass reactor equipped with a mechanical stirrer, a nitrogen inlet, and a Dean-Stark (D-S) apparatus with a condenser. The apparatus was immersed in a silicon oil bath and initially heated from 120 to 200°C for 1 h under nitrogen atmosphere to limit the evaporation of BDO during the formation of the first oligomers. Then, a temperature of 200°C was applied for 1 h under nitrogen atmosphere. In the second step of the reaction, vacuum was gradually applied over a 20 min time period, after which the temperature was maintained at 200°C for 2 h. Finally, the temperature was raised to 220°C to increase the molar mass of the resulting PBS.

Techniques

Size Exclusion Chromatography. Molar masses of PBS studied in rheology were obtained by size exclusion chromatography (SEC) using a Waters HPLC system equipped with a Waters 600 HPLC pump, a Waters 710plus automated injector, a Jasco CO-965 column oven, a Waters 410 Refractive Index (RI) detector, and a set of two PLgel 5 μm MIXED-D columns 300 × 7.5 mm. Chloroform was used as eluent at a flow rate of 1 mL min^{-1}, and an approximate sample concentration of 1.5 mg mL^{-1} was used. Polystyrene standards were employed for the calibration curve. The oven and the RI cell temperature were set at 35°C. Samples were filtered through a 0.45-μm poly(tetrafluoroethylene) (PTFE) membrane prior to be injected.

Rheological Properties. Rheological properties of PBS were studied using an AR 2000 ex Rheometer (TA Instruments) with parallel plate geometry of 25 mm diameter and a gap of 1 mm. The rheological measurements were carried out in the angular frequency range of 100–0.1 rad s^{-1}, and each sample was studied at five different temperatures: 120, 130, 140, 150, and 160°C with a constraint strain of 10%. The constraint strain was determined after a prior strain sweep study at an angular frequency of 10 rad s^{-1} in order to estimate the Linear Viscoelastic Region (LVR) of the samples. All samples analyzed in the temperature range of 120–140°C were first heated at 150°C for 5 min and cooled to the desired temperature in order to remove any crystalline fraction. The samples were first dried in an oven overnight at 60°C before each measurement. The closure of the gap was carried out exponentially to avoid breaking the structure of samples.

Dilute Solution Properties. A size exclusion chromatography-triple detection (SEC-TD) was used for dilute solution analysis of PBS in chloroform. The system was equipped with a 390-LC Multi Detector Suite (Varian) with a 290-LC pump (with an injection valve and an online degassor module), a GPC PS 510 column oven, a 390-LC refractive index detector, a 390-LC four-capillary viscometer detector, a 390-LC two-angle light scattering (15° and 90°; $\lambda = 650$ nm) detector, and a set of two PLGel 5 μm MIXED-D columns 300 × 7.5 mm. Chloroform was employed as eluent at a flow rate of 1 mL min^{-1}, and an approximate sample concentration of 2 mg mL^{-1} was used. Eluent was filtered through a 0.2-μm PTFE membrane before using. The oven and detectors temperature were set at 30°C. Samples were filtered through a 0.45-μm PTFE membrane prior to be injected.

RESULTS AND DISCUSSION

Influence of Molar Mass on the Rheological Properties of PBS

Frequency Sweep. Melt-rheological properties of PBS with different molar masses (Table I) were characterized by a parallel plate rheometer. Each sample was studied at five different temperatures: 120, 130, 140, 150, and 160°C. The temperature influence on the storage modulus G' and the loss modulus G'' of sample PBSh is shown in Figure 1. As can be seen, for a given frequency, the increase in temperature decreases the value of both $G'$and G''.

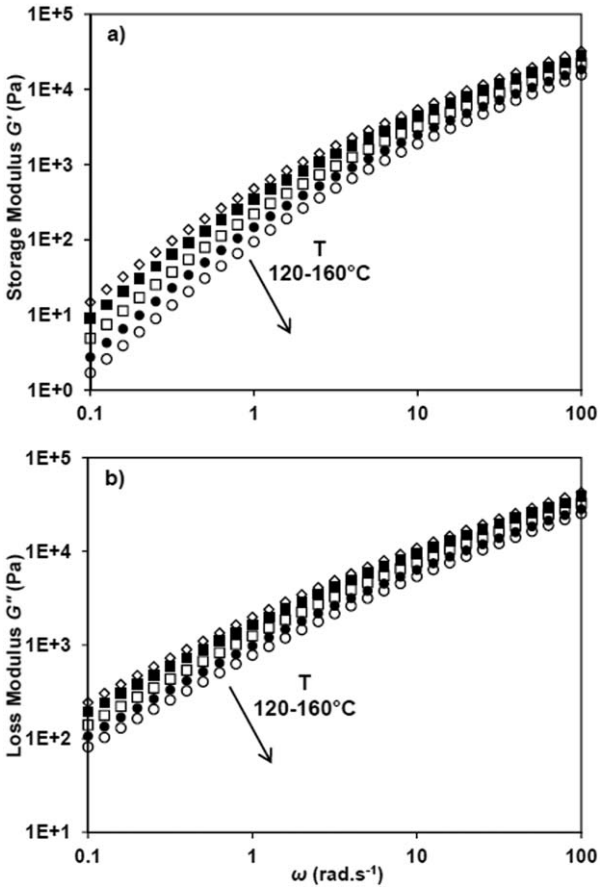

Figure 1. Temperature influence on (a) storage modulus G' and (b) loss modulus G'' versus angular frequency of PBSh.

We observed that the sample reaches its terminal region at a higher frequency value when temperature increases, meaning that the relaxation time decreases. A similar behavior was observed for the samples PBSd to PBSi. We measured a constant G'' slope for the samples PBSa to PBSc for each temperature in the frequency range studied. In addition, the G' curves of these three samples showed no linear behavior. These results can be explained by a phase angle δ, between the complex stress and the complex strain, higher than 89°, meaning that the elastic component of the complex modulus $G^{\star}$ is insignificant compared to the viscous component.

Therefore, results of all samples will be presented at the reference temperature $T_0 = 140°C$, by applying the Temperature–Time Superposition (TTS) principle to the experimental data. The master curves of the reduced plots of the storage modulus G_r' and the loss modulus G_r'' versus ωa_T, where a_T is a temperature-dependent shift factor, are presented in Figure 2.

As can be seen, G_r' and G_r'' moduli increase when molar mass increases. We can also note a great scattering and a decrease in the G_r' slope, for the samples PBSd to PBSg, when the frequency becomes lower than 1 rad s^{-1}, while G_r'' slope is still constant. Here again, this behavior is due to a phase angle higher than 89°.

These data show that all samples reach the terminal region in the frequency range studied. This phenomenon is illustrated by the slope change of moduli G_r' and G_r'' between the high and low frequency areas for the samples PBSd to PBSi. This result is a first sign of the presence of entanglements within these samples. As can be seen, increasing molar mass decreases the frequency at which PBS enters in its terminal region. In other words, the relaxation time of PBS increases as molar mass increases. However, curves of modulus G_r'' for samples PBSa to PBSc show that samples are in the terminal zone in the entire frequency range studied, which means that there is no entanglement within these three samples. Finally, in the terminal region, the slope of $\log G_r''$ versus $\log \omega a_T$ is equal to 1 for all samples, while the slope of $\log G_r'$ versus $\log \omega a_T$ is equal to 2 for PBSi and equal to 1.9 for the samples from PBSd to PBSh, which is in agreement with theory.[23]

The Complex Viscosity. Determination of the complex viscosity $|\eta^*|$ was carried out from frequency sweep analyses. The Cox–Merz equality suggests that, for a neat polymer, complex viscosity $|\eta^*|$ is almost equal to shear viscosity $\eta(\dot{\gamma})$.[23,24] Assuming that the Cox–Merz equality can be applied to our samples, Figure 3 represents the viscosity η versus the shear rate $\dot{\gamma}$ for the samples PBSd to PBSi at 140°C. Samples PBSa to PBSc behave like Newtonian fluids. As can be seen, for a given shear rate $\dot{\gamma}$, η increases when M_w increases. Non-Newtonian behavior of samples PBSd to PBSi confirms the presence of entanglements within these samples. Figure 3 also shows that the data fit very

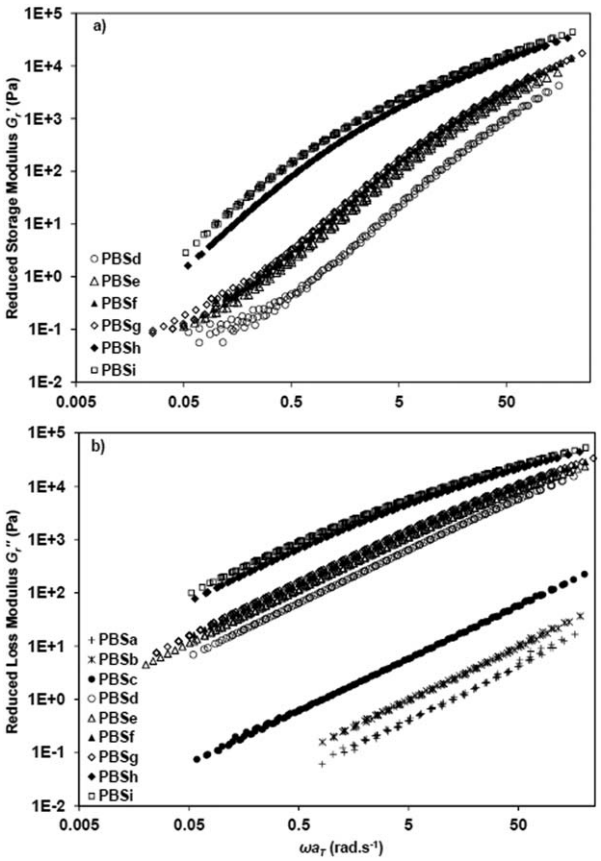

Figure 2. Master curves of reduced (a) storage modulus G_r' and (b) loss modulus G_r' versus ωa_T of PBSs at 140°C.

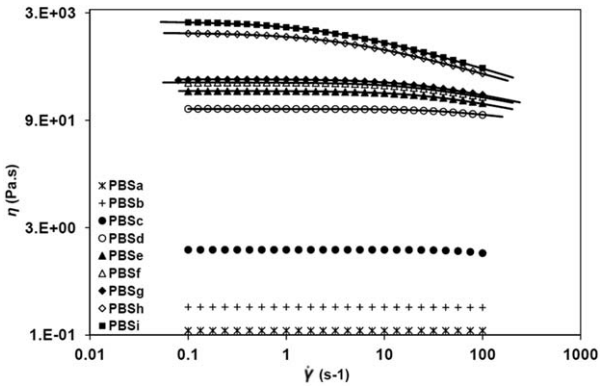

Figure 3. Viscosity η versus shear rate $\dot{\gamma}$ of PBS samples at 140°C. Black lines are the fitting of the Carreau–Yasuda model.

well with the Carreau–Yasuda model (black lines), which is defined by the following relationship:

$$\eta = \eta_0(1+(\lambda\dot{\gamma})^a)^{\frac{m-1}{a}} \quad (1)$$

where λ is a characteristic transition time between the Newtonian and the pseudoplastic region, m is the index of pseudoplasticity ($m=1$ for Newtonian fluid and $m=0$ for a rigid solid) and a is an adjustment coefficient between the Newtonian plateau and the power law region. All these parameters and the zero-shear viscosity η_0 are given in Table I.

As expected, relaxation time λ, reflecting the time of disentanglement of a polymer, increases when M_w increases. In addition, the decrease in m highlights the non-Newtonian behavior of PBS with the increase in M_w. Finally, a good correlation was found between the zero-shear viscosity η_0 calculated from the Carreau–Yasuda model and the one calculated from the following relationship:

$$\eta_0 = \lim_{\omega\to 0} G_r''/\omega \quad (2)$$

Wang et al.[13] found a η_0 situated between 800 and 900 Pa s for a PBS with a M_w of 142,000 g mol^{-1} at 140°C. By comparison, we measured a η_0 of 1410 Pa s for a M_w of 146,400 g mol^{-1}.

A very well-known relationship connects the zero-shear viscosity η_0 of a molten polymer to its molar mass M_w: $\eta_0 = KM_w^{\alpha}$, where K is a constant depending on the nature of the polymer.[25] According to theory and numerous experimental data in literature, η_0 changes in two different regimes separated by a critical molar mass M_c.[23,25] In theory, when $M_w < M_c$, η_0 is proportional to M_w ($\alpha = 1$). In practice, α can be between 1 and 2.5. And when $M_w > M_c$, η_0 becomes theoretically proportional to $M_w^{3.4}$. Many experimental data showed that α can be between 3.4 and 3.7.[26]

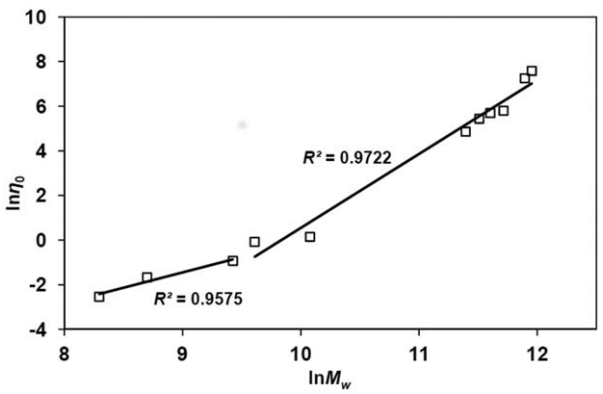

Figure 4. $\ln\eta_0$ versus $\ln M_w$ of PBS samples. Dashed lines and black lines are the linear fitting used to estimate M_c.

Figure 4 shows the experimental data of $\ln\eta_0$ versus $\ln M_w$ for all samples studied. Two more samples ($M_w = 12{,}400$ and 14,900 g mol^{-1}, respectively), synthesized under the same protocol described in the experimental part of this article, were added in order to complete the area of low molar mass.

As expected, we observe two distinct domains from these experimental data. M_c was estimated from the linear fittings of these two domains. The first linear fitting corresponds to the low molar mass region comprised between 4000 and 12,400 g mol^{-1} where $\ln\eta_0 = 1.37 \times \ln M_w - 13.804$. The second domain corresponds to the high molar mass region and is situated between 14,900 and 155,400 g mol^{-1} where $\ln\eta_0 = 3.31 \times \ln M_w - 32.595$. The values of α are in agreement with the theory and the experimental data obtained for other polymers. Thus, we calculated a critical molar mass M_c of 16,000 g mol^{-1}. This value is in agreement with M_c mentioned in the literature for other aliphatic polyesters such as poly(lactic acid) (PLA) or poly(ε-caprolactone) (PCL). Indeed, M_c of PLA has been estimated between 9000 and 16,000 g mol^{-1},[27,28] while that of PCL has been estimated between 8000 and 16,000 g mol^{-1}.[29–31]

The Activation Energy E_a of Melt PBS. The activation energy E_a of melt PBS was calculated from temperature-dependent shift factor a_T, determined from the TTS principle. Under our experimental conditions, PBS is above its temperature of fusion and the reference temperature T_0 (140°C) is well above T_g+100°C ($T_g \approx -32$°C). Thus, the dependence between a_T and the temperature of experiment T (120, 130, 150, and 160°C) is defined by the Arrhenius law: $a_T = \exp(E_a/R(1/T - 1/T_0))$, where R is the gas constant. We used the shift factors obtained from the preparation of the loss modulus master curves G_r'', and E_a of each sample was calculated from the slope of the linear fitting of $\ln a_T$ versus $(1/T - 1/T_0)$. The linear regression was higher

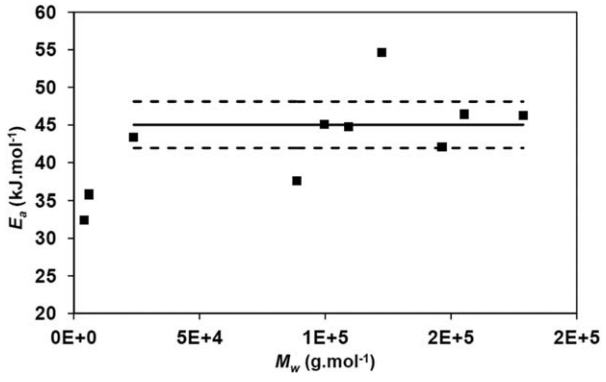

Figure 5. Activation energy E_a versus molar mass M_w (PS equivalent) of PBS samples. Black line is the average and dashed lines are the average deviation in the range $23{,}800 < M_w < 178{,}800$ g mol^{-1}.

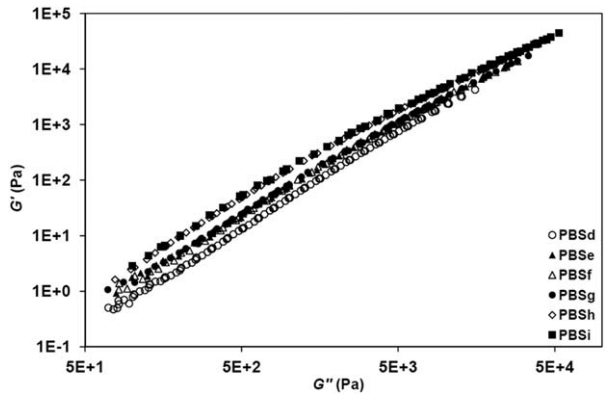

Figure 6. log G' versus log G'' of PBS samples.

than 0.99 for all samples (Supporting Information Figure S1). So E_a versus M_w is represented in Figure 5.

The two lowest E_a were attributed to the two samples with the lowest molar mass PBSa (4000 g mol^{-1}) and PBSb (6000 g mol^{-1}). We estimated an average energy $\bar{E}_a$ for the rest of the series: $\bar{E}_a = 45.02 \pm 3.09$ kJ mol^{-1}. The average energy and average deviation are represented by the solid line and the two dashed lines in Figure 5, respectively. As can be seen, two values fall outside the average deviation (88,800 and 122,400 g mol^{-1}). This average value $\bar{E}_a$ suggests that the activation energy of PBS melt is independent of molar mass for $M_w \geq 23{,}800$ g mol^{-1}.

This first observation is in agreement with experimental data found in literature about other polymers.[32,33] The activation energy of a molten polymer can be described as an energy barrier crossed by a segment of a definite size of the chain from an occupied site to an empty site.[34] In other words, it means that the flow of a polymer can be considered as a succession of elementary transition acts attributed to segments of the chain called flow segments. According to Siline and Leonov,[33] for high molar mass polymers, the length of the flow segment is less than the length of the polymer chain between entanglements. Moreover, it is well established that the molar mass between entanglements M_e is about one half of M_c, that is to say, $M_c \approx 2M_e$.[23,35] Taking into account the previously determined value of $M_c = 16{,}000$ g mol^{-1} and the lowest molar masses of the two samples, $M_w < M_e \approx 8000$ g mol^{-1}, we find an explanation for the respective $E_a < \bar{E}_a$ for these two samples.

Finally, the average activation energy calculated here is almost the same as the one found by Ray et al.[18] (42 kJ mol^{-1}) for a commercial PBS (Bionolle 1020) with a M_w of 101,000 g mol^{-1}.

Estimation of the Plateau Modulus G_N^0. The plateau region is one of the most important viscoelastic properties distinguishing entangled polymers from unentangled polymers. The plateau modulus G_N^0 is linked to the molar mass M_e as follows: $G_N^0 = \rho RT/M_e$ where ρ is the density of the polymer. In practice, there are several methods to determine G_N^0.[36] The easiest way is by visualizing directly this plateau on the storage modulus curve. But in this study, this region was not reached for several reasons, including measurement temperatures well above the glass transition temperature of PBS ($T_g \approx -32$°C) and insufficient molar masses. Han and Kim[37] reported a method to determine G_N^0 for polymolecular polymers from the evolution of $\log G'$ versus $\log G''$. In this case, there are two different linear evolutions of $\log G' = f(\log G'')$. The first part, the linear region where $0 << \tau_w\omega \leq 1$ (with τ_w the terminal relaxation time), is located toward the high values of G' and G'' and is defined by: $\log G' = x\log G'' + (1-x)\log\left(8G_N^0/\pi^2\right)$. The second part, the terminal zone where $\tau_w\omega << 1$, is located toward the low values of G' and G'' with a slope of 2. This behavior can be seen in Figure 6 for the samples PBSd to PBSi.

We observed two linear regions with different slopes. According to the previous estimation of M_e, entanglement effects are dominant for all samples in Figure 6. Also, these curves are independent of molar mass.[23]

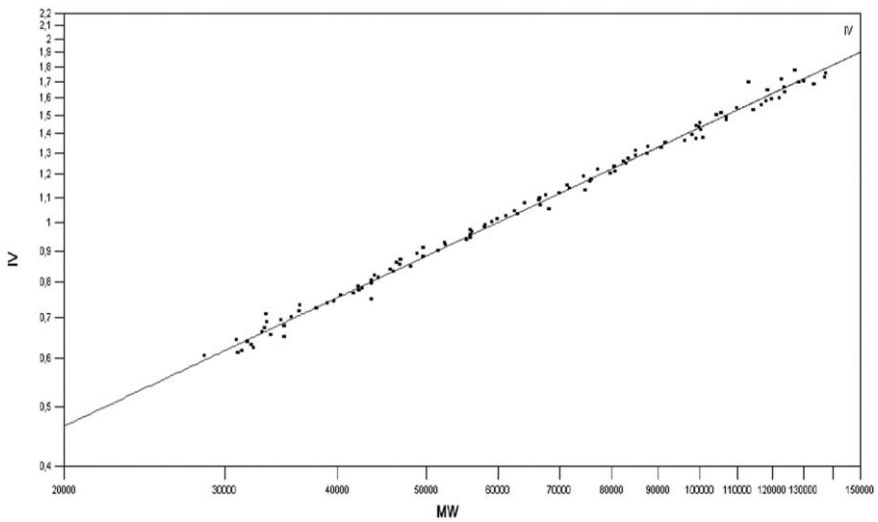

Figure 7. Intrinsic viscosity [η] versus molar mass M_w (black points) of PBS4 in the range $20{,}000 < M_w < 150{,}000$ g mol^{-1}. Black line is the linear fitting traced by software Cirrus.

Table II. Parameters of the Mark-Houwink-Sakurada Relationship of PBS Samples

Sample M_w range (g mol^{-1})	a_1	a_2	a_3	Average a	$K_1 \times 10^5$ (dL g^{-1} (g mol^{-1})$^{-a}$)	$K_2 \times 10^5$ (dL g^{-1} (g mol^{-1})$^{-a}$)	$K_3 \times 10^5$ (dL g^{-1} (g mol^{-1})$^{-a}$)	Average $K \times 10^5$ (dL g^{-1} (g mol^{-1})$^{-a}$)
PBS1 25,000-70,000	0.693	0.725	0.736	0.718	43.12	29.67	29.323	33.138
PBS2 24,000-90,000	0.724	0.716	0.729	0.723	33.748	38.266	31.882	34.632
PBS3 30,000-130,000	0.702	0.711	0.702	0.705	44.814	38.87	48.562	44.085
PBS4 30,000-140,000	0.682	0.698	0.703	0.694	50.366	46.05	44.61	47.012

The shift occurring between these curves is due to the difference in I_p of these samples (Table I). Indeed, the curves overlap for samples with the same I_p but different M_w. This is the case for two groups composed of PBSe, PBSf, and PBSg on the one hand and of PBSh and PBSi on the other hand. In theory, the increase in I_p decreases the slope x of the linear region. This was confirmed by the decrease in x from 1.59 to 1.32, while I_p increases from 2.16 to 2.47 (Table I). Even if these first observations are in agreement with theory, we only observed a nearly constant value of G_N^0 at an average of 1.51×10^5 Pa for samples PBSd to PBSg. G_N^0 of PBSh and PBSi decrease because these two samples are not under the required conditions: $0 << \tau_w\omega \leq 1$. Indeed, we determined a terminal relaxation time τ_w of 0.53 s for PBSi with the equation $\tau_w = \eta_0 J_e^0$, where J_e^0 is the steady-state compliance. Thus, sample PBSi is almost out of the conditions of the equation proposed by Han and Kim.[37] The terminal relaxation time of PBSh was not determined but the evolutions of G_r' and G_r'' are fairly close to those of PBSi. So, it can be assumed that this sample is also almost outside of the equation conditions. Finally, the G_N^0 average of 1.51×10^5 Pa is in the same range as the ones reported for other biodegradable aliphatic polyesters like PLA: 0.9×10^5 and 2.03×10^5 Pa or like PCL: 1.46×10^5 and 5.52×10^5 Pa.[38]

Dilute Solution Properties of PBS in Chloroform

A SEC with the triple detection system (SEC-TD) was used to determine the MHS parameters of PBS in solution in chloroform at 30°C. The MHS relationship is defined by: $[\eta] = KM_v{}^a$, where the MHS parameters K and a are dependent on a given polymer–solvent couple and on the measurement temperature. The exponent a gives information about the conformation of the polymer studied in solution. a is between 0 and 0.5 for a branched polymer, between 0.5 and 0.8 for flexible chains, between 0.8 and 1 for stiff molecules, and between 1 and 1.7 for highly extended macromolecules.[39] Moreover, a is 0.5 at unperturbed state (Θ condition) and is 0.8 for a polymer in a good solvent. Finally, considering the non-Gaussian character of small chains, the MHS relationship can only be applied for a polymer with a molar mass higher than 20,000 g mol^{-1}.[40]

Generally, MHS parameters are determined by measuring intrinsic viscosity $[\eta]$ on the one hand and molar mass M_w on the other hand. However, for polydisperse polymers such as PBS, viscosity and weight average molar masses, M_v and M_w respectively, are not exactly the same. This can lead to an error in the estimation of the MHS parameters. Thus, SEC-TD allows determining simultaneously the absolute molar mass and the intrinsic viscosity of a polymer for each elution fraction. This last point is very interesting because each elution fraction is composed of an isomolecular population.

Samples used for the dilute solution properties study are issued from a different synthesis series than the ones used for the rheological properties. Here, samples are named PBSi, with $i = 1$ to 4. Figure 7 represents $\log[\eta] = f(\log M_w)$ of PBS4.

The MHS parameters are calculated by the software Cirrus from the linear fitting (black line) of the experimental data. In this example, the values of a and K are 0.698 and 46.05×10^{-5} dL g^{-1}(g mol^{-1})$^{-a}$, respectively. Parameters calculated for all samples are grouped in Table II. Three injections per sample were realized because dead volume between detectors can be a source of error for MHS parameters determination.[41]

On the whole, the MHS parameters are consistent for all samples. A small increase in K of the two samples PBS3 and PBS4 could be observed. Thus, the average MHS parameters of PBS in chloroform at 30°C were calculated: $a = 0.71 \pm 0.1$ and $K = 39.94 \times 10^{-5} \pm 6.31 \times 10^{-5}$ dL g^{-1}(g mol^{-1})$^{-a}$. As expected, the value of a confirms the statistical coil behavior of PBS in solution in chloroform. As an estimation of the MHS parameters was not yet reported in the literature, we could only compare these values with those of other aliphatic polyesters such as PLA and PCL. For example, exponent a of PLA in solution in chloroform at 30°C was estimated at 0.777.[42] However, there is a disagreement on the estimation of exponent a of PLA because values between 0.72 and 0.83 have also been reported at 25°C.[43] Several values are also available in the literature for PCL in solution in chloroform: 0.786 (25°C),[44] 0.71 (25°C),[45] and 0.828 (30°C).[46]

CONCLUSIONS

First, we studied the influence of molar mass on the rheological properties of PBS. We were able to apply the TTS principle from the data obtained with frequency sweep measurements, and we observed a significant increase in modules G' and G'' when molar mass increases. In addition, shear viscosity of PBS followed the Carreau–Yasuda relationship. Two fundamental parameters which are not reported in the literature were estimated in this study: the critical molar mass for entanglement $M_c = 16{,}000$ g mol^{-1} and the plateau modulus $G_N^0 = 1.51 \times 10^5$ Pa. These two values are close to the ones reported for other aliphatic polyesters such as PLA and PCL. Finally, average activation energy of PBS melt ($\bar{E}_a = 45.02 \pm 3.09$ kJ mol^{-1}) was calculated for molar masses between 23,800 and 178,800 g mol^{-1}.

In the second part of this study, we estimated values of the MHS parameters of PBS in solution in chloroform at 30°C. This was achieved with a SEC-TD from which we obtained values of the couple $[\eta]$–M_w for each elution fraction of the samples. Thus, from three injections for each one of four samples studied, we obtained the following average values for the MHS parameters: $a = 0.71 \pm 0.1$ and $K = 39.94 \times 10^{-5} \pm 6.31 \times 10^{-5}$ dL g^{-1}(g $mol^{-1})^{-a}$.

ACKNOWLEDGMENTS

This work has been financially supported by Conseil Régional Champagne-Ardenne, in the scope of the research project MATOREN, to whom the authors express their gratitude.

REFERENCES

1. Baytekin, B.; Baytekin, H. T.; Grzybowski, B. A. *Energ. Environ. Sci.* **2013**, *6*, 3467.
2. Avérous, L.; Pollet, E. In Environmental Silicate Nano-Biocomposites; Avérous, L.; Pollet, E., Eds.; Springer: London, **2012**; p 13.
3. Scott, G. *Polym. Degrad. Stab.* **2000**, *68*, 1.
4. Ling, E. T.; Dibble, J. T.; Houston, M. R.; Lockwood, L. B.; Elliott, L. P. *Appl. Environ. Microbiol.* **1978**, *35*, 1213.
5. Rossi, C.; Hauber, J.; Singer, T. P. *Nature* **1964**, *204*, 167.
6. Bechthold, I.; Bretz, K.; Kabasci, S.; Kopitzky, R.; Springer, A. *Chem. Eng. Technol.* **2008**, *31*, 647.
7. Song, H.; Lee, S. Y. *Enzyme Microb. Technol.* **2006**, *39*, 352.
8. Xu, J.; Guo, B.-H. In Plastics from Bacteria; Chen, G. G.-Q., Ed.; Springer: Berlin Heidelberg, **2010**; Vol. *14*, p 347.
9. Xu, J.; Guo, B.-H. *Biotechnol. J.* **2010**, *5*, 1149.
10. BDO/THF. http://www.bio-amber.com/bioamber/fr/products/bdo_thf (Accessed March 7, 2012).
11. Cukalovic, A.; Stevens, C. V. *Biofuel Bioprod. Bioref.* **2008**, *2*, 505.
12. Yim, H.; Haselbeck, R.; Niu, W.; Pujol-Baxley, C.; Burgard, A.; Boldt, J.; Khandurina, J.; Trawick, J. D.; Osterhout, R. E.; Stephen, R.; Estadilla, J.; Teisan, S.; Schreyer, H. B.; Andrae, S.; Yang, T. H.; Lee, S. Y.; Burk, M. J.; Van Dien, S. *Nat. Chem. Biol.* **2011**, *7*, 445.
13. Wang, G.; Guo, B.; Li, R. *J. Appl. Polym. Sci.* **2011**, *124*, 1271.
14. Wang, G.; Guo, B.; Xu, J.; Li, R. *J. Appl. Polym. Sci.* **2011**, *121*, 59.
15. Ali, F. B.; Mohan, R. *Polym. Compos.* **2010**, *31*, 1309.
16. Han, S.-I.; Lim, J. S.; Kim, D. K.; Kim, M. N.; Im, S. S. *Polym. Degrad. Stab.* **2008**, *93*, 889.
17. Okamoto, K.; Sinha Ray, S.; Okamoto, M. *J. Polym. Sci. Part B: Polym. Phys.* **2003**, *41*, 3160.
18. Ray, S. S.; Okamoto, K.; Okamoto, M. *J. Appl. Polym. Sci.* **2006**, *102*, 777.
19. Sinha Ray, S.; Okamoto, K.; Okamoto, M. *Macromolecules* **2003**, *36*, 2355.
20. Kim, Y. J.; Park, O. O. *J. Appl. Polym. Sci.* **1999**, *72*, 945.
21. Yokohara, T.; Yamaguchi, M. *Eur. Polym. J.* **2008**, *44*, 677.
22. Li, G.; Qi, R.; Lu, J.; Hu, X.; Luo, Y.; Jiang, P. *J. Appl. Polym. Sci.* **2013**, *127*, 3586.
23. Dae Han, C. Rheology and Processing of Polymeric Materials; Vol. *1*: Polymer Rheology; Oxford University Press, **2007**.
24. Mobuchon, C.; Carreau, P. J.; Heuzey, M. C.; Sepehr, M.; Ausias, G. *Polym. Compos.* **2005**, *26*, 247.
25. Graessley, W. W., *Adv. Polym. Sci.* **1974**, *16*, 1.
26. Ressia, J. A.; Villar, M. A.; Vallés, E. M. *Polymer* **2000**, *41*, 6885.
27. Cooper-White, J. J.; Mackay, M. E. *J. Polym. Sci. Part B: Polym. Phys.* **1999**, *37*, 1803.
28. Dorgan, J. R.; Janzen, J.; Clayton, M. P.; Hait, S. B.; Knauss, D. M. *J. Rheol.* **2005**, *49*, 607.
29. Gimenez, J.; Cassagnau, P.; Fulchiron, R.; Michel, A. *Macromol. Chem. Phys.* **2000**, *201*, 479.
30. Grosvenor, M. P.; Staniforth, J. N. *Int. J. Pharm.* **1996**, *135*, 103.
31. Noroozi, N.; Thomson, J.; Noroozi, N.; Schafer, L.; Hatzikiriakos, S. *Rheol. Acta* **2012**, *51*, 179.
32. Shen, L.; Song, Y.-H.; Qian, Y.-J.; Qiao, F.; Zhang, J.-L.; Zheng, Q. *Chin. J. Polym. Sci.* **2008**, *26*, 639.
33. Siline, M.; Leonov, A. I. *Polymer* **2002**, *43*, 5521.
34. Kauzmann, W.; Eyring, H. *J. Am. Chem. Soc.* **1940**, *62*, 3113.
35. Ferry, J. D. Viscoelastic Properties of Polymers, 3rd ed.; Wiley, New York, **1980**.
36. Liu, C.; He, J.; Ruymbeke, E. V.; Keunings, R.; Bailly, C. *Polymer* **2006**, *47*, 4461.
37. Han, C. D.; Kim, J. K. *Macromolecules* **1989**, *22*, 4292.
38. Ramkumar, D. H. S.; Bhattacharya, M. *Polym. Eng. Sci.* **1998**, *38*, 1426.
39. Massey, J. A.; Kulbaba, K.; Winnik, M. A.; Manners, I. *J. Polym. Sci. Part B: Polym. Phys.* **2000**, *38*, 3032.
40. Gnanou, Y.; Fontanille, M. In Chimie et physico-chimie des polymères 2e Edition; Dunod.
41. Zammit, M. D.; Davis, T. P. *Polymer* **1997**, *38*, 4455.
42. Dorgan, J. R.; Janzen, J.; Knauss, D. M.; Hait, S. B.; Limoges, B. R.; Hutchinson, M. H. *J. Polym. Sci. Part B: Polym. Phys.* **2005**, *43*, 3100.
43. Garlotta, D. *J. Polym. Environ.* **2001**, *9*, 63.
44. Celiz, A. D.; Scherman, O. A. *Macromolecules* **2008**, *41*, 4115.
45. Sabino, M. A. *Polym. Degrad. Stab.* **2007**, *92*, 986.
46. Xiao, X.; Liu, R.; Huang, Q.; Ding, X. *J. Mater. Sci. Mater. Med.* **2009**, *20*, 2375.